Bending leaves and flapping flight

Transitions in fluid-structure interactions

Silas Alben
Harvard DEAS

Advisor:
Michael Shelley
NYU Math

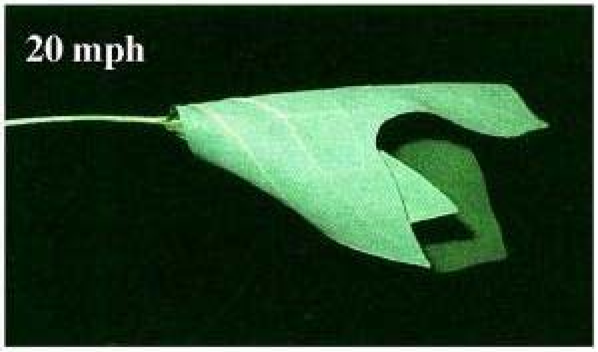

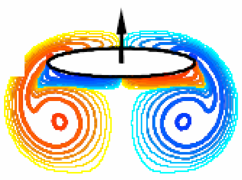

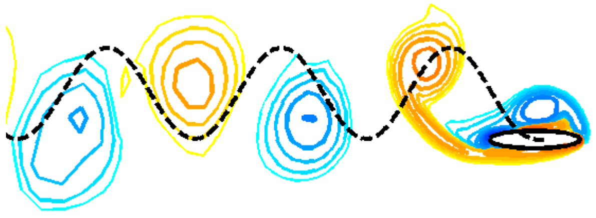

Scaling of fluid drag vs. flow speed for various plants

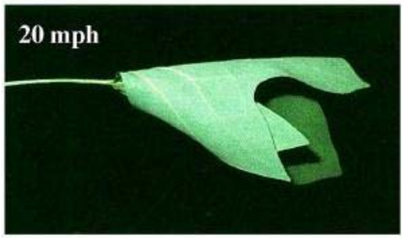

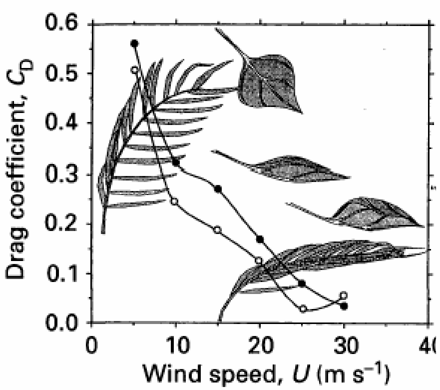

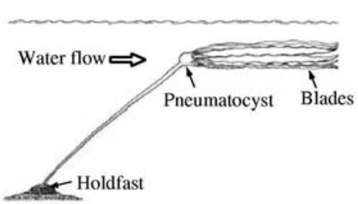

Vogel, *Life in Moving Fluids*

$D \sim U^{2+E}$

System	*Re or Speed Range*	E	*Source of Data*
Bluff body	<1.0	−1.00	
Bluff body	1000–200,000	0.00	
Flat plate, parallel to flow	10–1000	−0.60	Janour 1951
Flat plate, parallel to flow	1000–500,000	−0.50	
Streamlined body, laminar flow	1000–500,000	−0.50	
Cylinder, axis normal to flow	20–120	−0.29	White 1974
Hedophyllum sessile (alga)	0.5–2.5 m/s	−1.12	Armstrong 1989
Nereocystis luetkeana (alga)	1.3–2.0 m/s	−1.07	Koehl & Alberte 1988
Sargassum filipendula (alga)	0.5–1.5 m/s	−1.47	Pentcheff (pers. comm.)
Laminaria (alga) on mussels	0.12 to 0.62 m/s	−1.40*	Witman & Suchanek 1984
Macroalgae, marine	ca. 2.5 m/s	−0.28 to −0.76	Carrington 1990
Red algae, freshwater	0.2–0.75 m/s	−0.33 to −1.27	Sheath & Hambrook 1988
Pinus sylvestris (pine)	9–38 m/s	−0.72*	Mayhead 1973
Pinus taeda, 1 m high	8–19 m/s	−1.13	Vogel 1984
Pinus taeda, branch	8–19 m/s	−1.16	"
Quercus alba (white oak), leaf	10–20 m/s	+0.97	Vogel 1989
Quercus alba, clustered leaves	10–20 m/s	−0.44	"
Other broad leaves & clusters	10–20 m/s	−0.20 to −1.18	"
Ptilosarcus gurneyi (sea pen)	0.11–0.26 m/s	−1.14	Best 1985
Pseudopterogorgia (gorgonian)	0.13–0.35 m/s	−1.66	Sponaugle & LaBarbera 1991
Abietenaria (hydroid)	0.025–0.40 m/s	−1.28*	Harvell & LaBarbera 1985
Acropora reticulata (hard coral)	1.5–3.0 m/s	+0.26*	Vosburgh 1982
Various limpet shells	0.15–0.45 m/s	0.0 to +1.2	Dudley 1985
Epeorus sylvicole (mayfly larva)	0.4–1.2 m/s	+0.28*	Weissenberger et al. 1991
Simulium vittatum (blackfly larva)	0.1–0.7 m/s	−0.64*	Eymann 1988
Locusta migratoria, antenna	20–120	−0.56	Gewicke & Heinzel 1980

NOTE: Asterisks indicate my calculations from published graphs.

A more controlled experiment: 1-D Leaf in a 2-D Flow

Flexible fiber in soap film

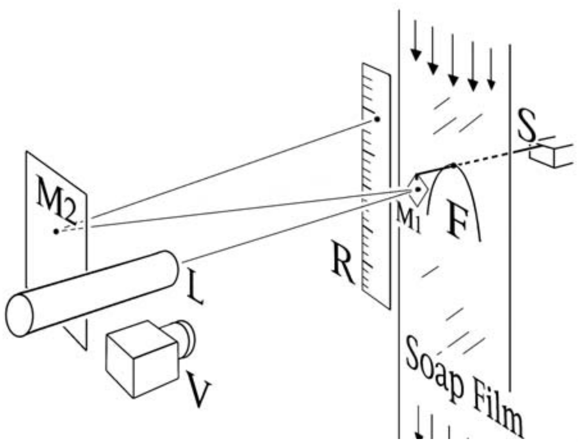

U = 0.7 m/s 1.4 m/s Re ~ 10^4

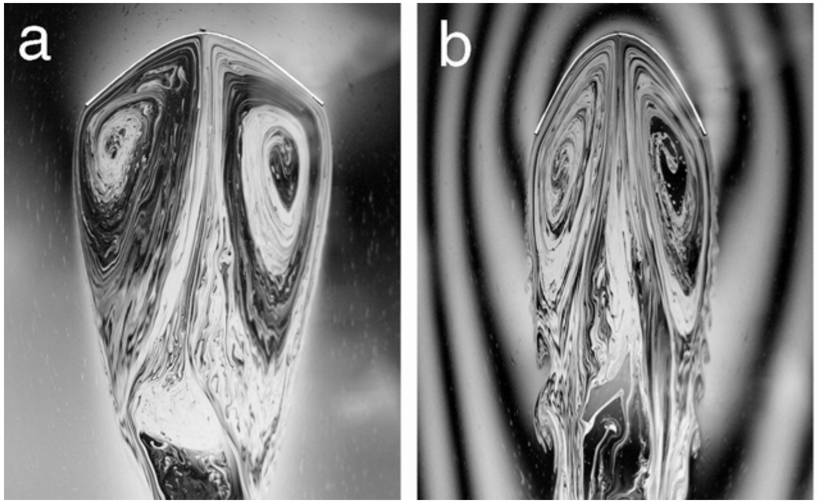

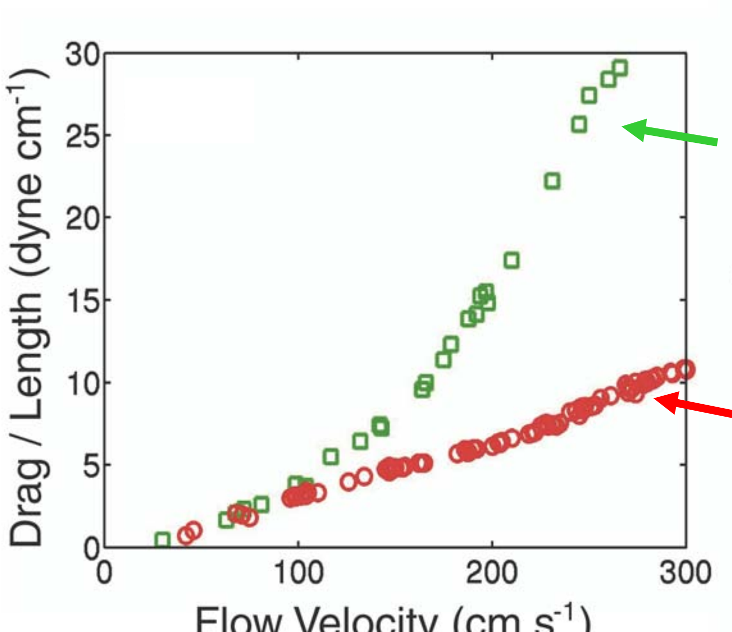

Rigid-body drag ~ U^2

Flexible-body drag ~ $U^?$

A Free-Streamline Model for the Flow Past a Bluff Body

In the flow:

$$p + (|\mathbf{u}|^2 - 1) = 0$$

$$\mathbf{u} = \nabla \phi$$

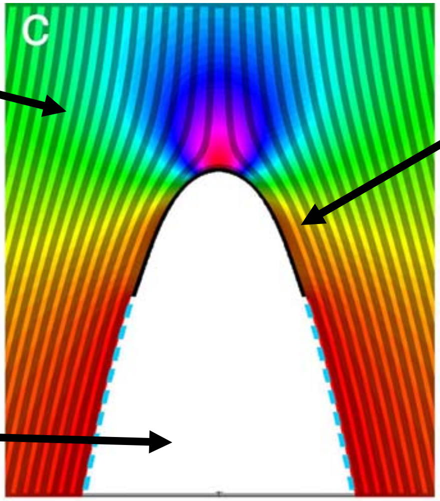

Fiber as an Elastica:

$$\theta_{sss} + \frac{1}{2}\theta_s^{\,3} = \eta^2 p$$

bending

tensile

fluid pressure

In the wake:

$$\mathbf{u} = 0,\ p = 0$$

$$\eta^2 = \frac{(1/2)\rho U^2 L^2 t}{B/L} = \frac{\text{Fluid kinetic energy}}{\text{Elastic energy}}$$

Numerical Solutions vs. Experiment

Shapes vs. Flow speed

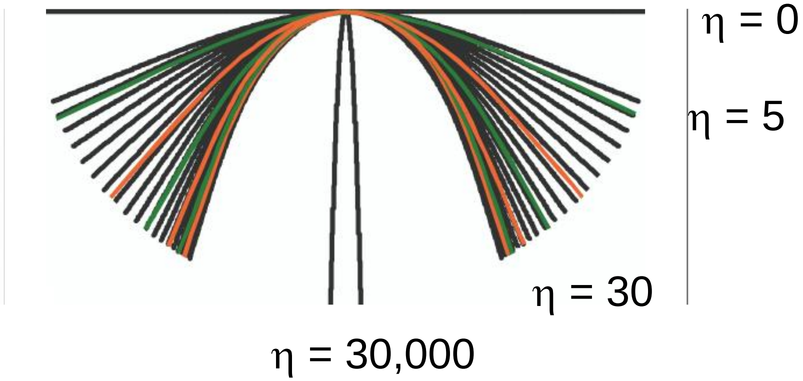

Scale distance from tip by $\eta^{-2/3}$:

Theory

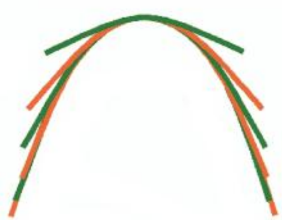

Experiment

Self-similar

Drag vs. Flow speed

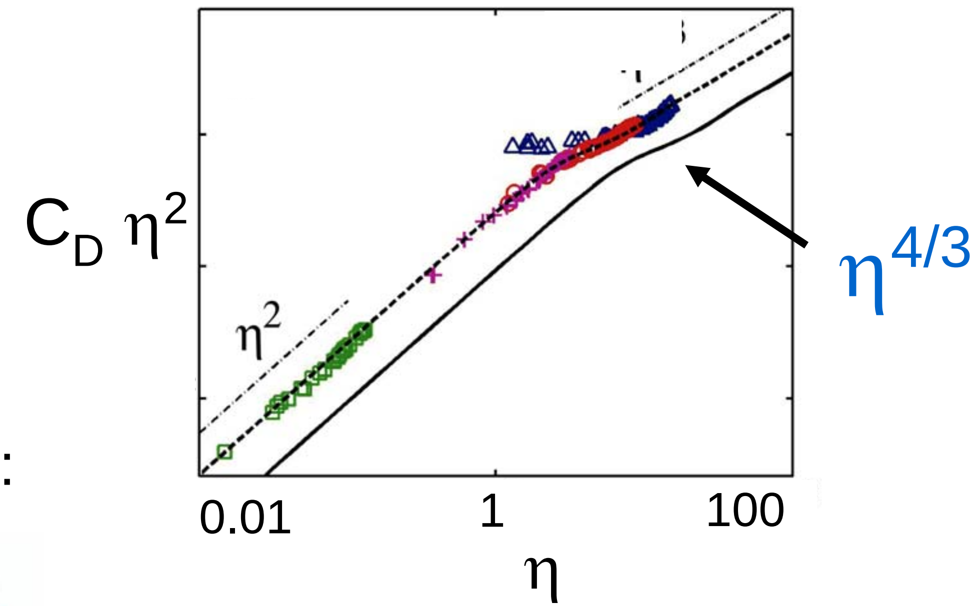

(ASZ, Nature '02)

How the length scale $\eta^{-2/3}$ arises

Uniform flow, folded fiber
is singular limit as $\eta \to \infty$

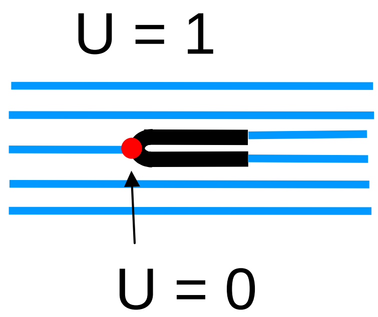

→ small tip scale

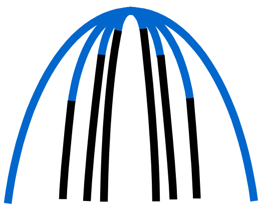

$$\theta = \Theta(s/\underline{\eta^{-\alpha}}) \qquad p = P(s/\underline{\eta^{-\alpha}})$$

collapsing length scales

$$\theta_{sss} + \frac{1}{2}\theta_s^3 = \eta^2 p \quad \to \underline{\alpha = 2/3}$$

Set $S \equiv s/\eta^{-2/3}$

The length scale explains:

1. $\eta^{4/3}$ drag, set by the tip region

$$\mathrm{Drag}_{\mathrm{tip}} = \eta^2 \int_{tip} p \; dy$$

$$= \eta^{4/3} \int_{tip} (\theta_{sss} + \frac{\theta^3}{2}) \sin\theta \; dS \sim \eta^{4/3}$$

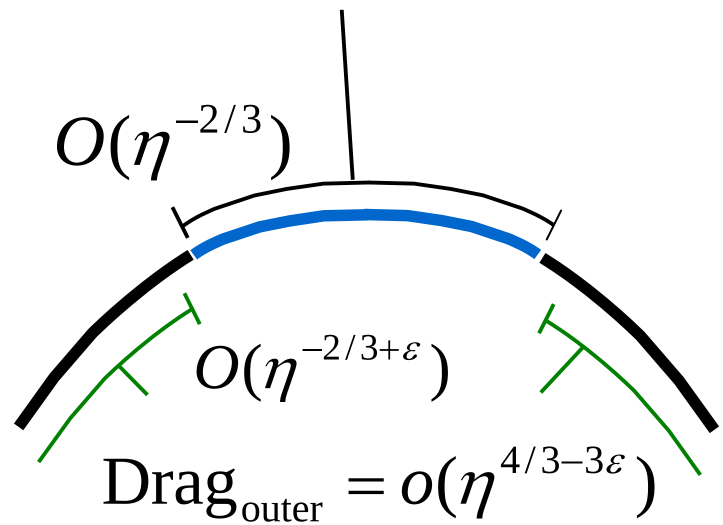

subdominant

2. body and wake asymptote to same parabolic shape

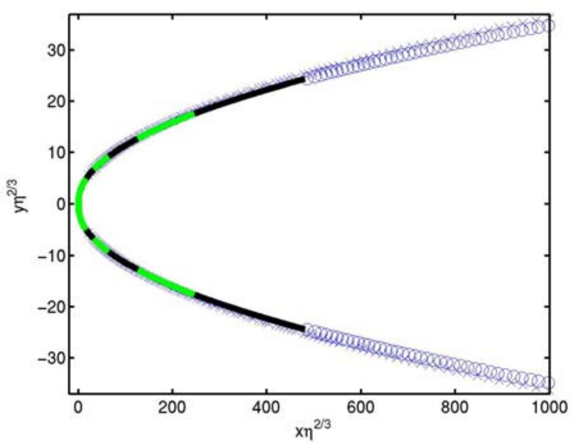

Summary

Model for drag reduction from flexibility
in a 2-D high-Re flow

Shapes are self-similar with $\eta^{-2/3}$ scale

Drag ~ $\eta^{4/3}$

Body and wake quasi-parabolic
("body sits inside wake of tip region")

Solutions have form:

$$\Theta(S) \sim C_1 S^{-1/2} + C_2 \eta^{-1} \cos(2^{1/3} S + \phi) + \ldots$$

Other wake models lead to the same scalings

Forward flight as an attracting state of vertical flapping

$$\mathrm{Re} = \frac{\rho L U}{\mu} = 0:$$ time-reversible motions do not generate locomotion

"Scallop theorem" from linearity of Stokes equations

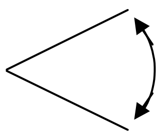

Re = 0:

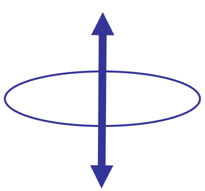

Re >> 1: (e.g. birds, fish, insects)

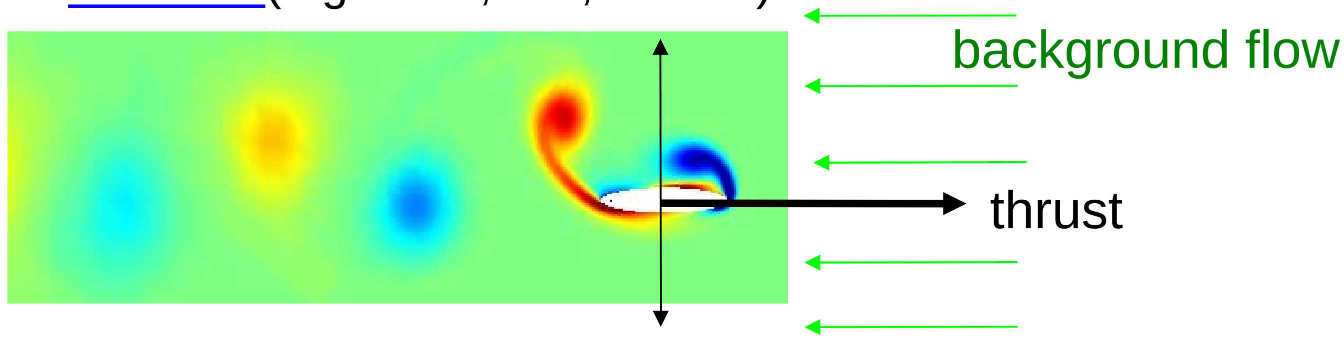

Reciprocal flapping is used often for locomotion

We investigate the transition (bifurcation) between these states (vs. Re)

An experimental study in a rotational geometry

Vandenberghe, Zhang
and Childress, 2004

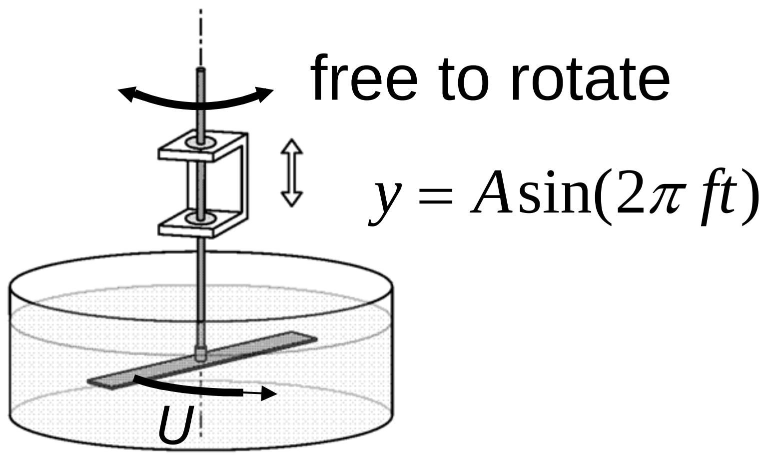

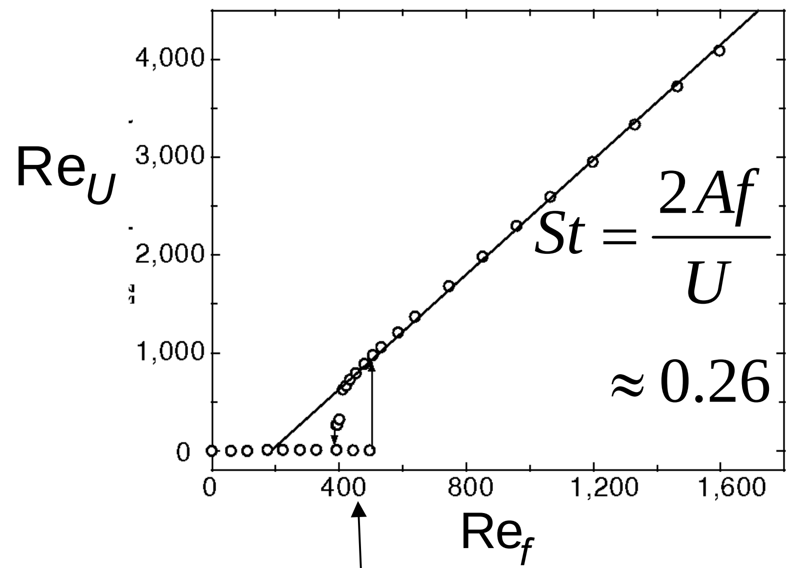

Near Re_{cr} :
Bistability, hysteresis

Set flapping speed $\mathrm{Re}_f = \dfrac{\rho LAf}{\mu}$,

Measure rotational speed $\mathrm{Re}_U = \dfrac{\rho LU}{\mu}$

Our 2D simulation to examine the transition

How do the fluid dynamics coordinate with the body motion?

Effect of body mass and shape?

Incompressible Navier-Stokes
coupled to Newton's Law

$$\frac{D\omega}{Dt} = \frac{1}{\mathrm{Re}_f}\Delta\omega$$

$$M\frac{dv_x}{dt} = \frac{1}{\mathrm{Re}_f}\hat{\mathbf{x}}\bullet\mathbf{F}_{\mathrm{fluid}}$$

$$y = A\sin(2\pi Aft)$$

Parameters: Re_f , $M = \frac{\rho_{body}}{\rho_{fluid}}$,

Aspect ratio

Solved with semi-implicit method

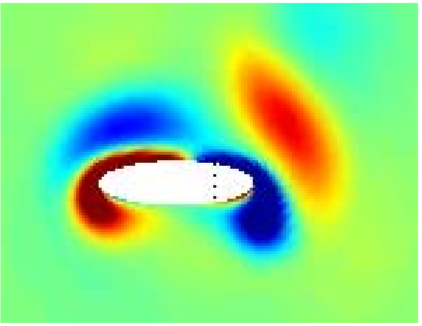

“Phase diagram” of states vs. M, Re_f

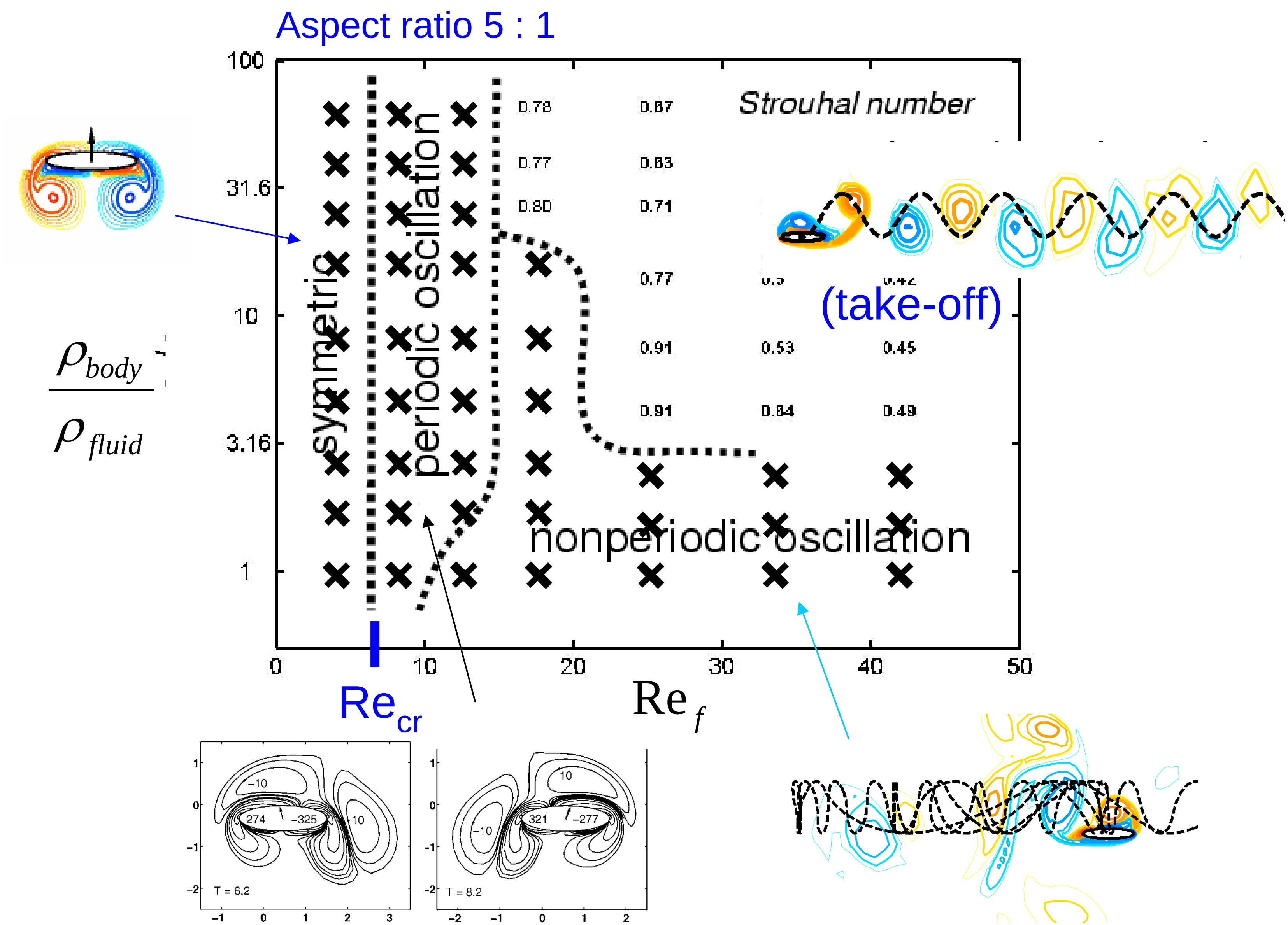

The sequence of events leading to forward flight

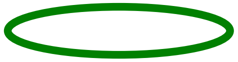

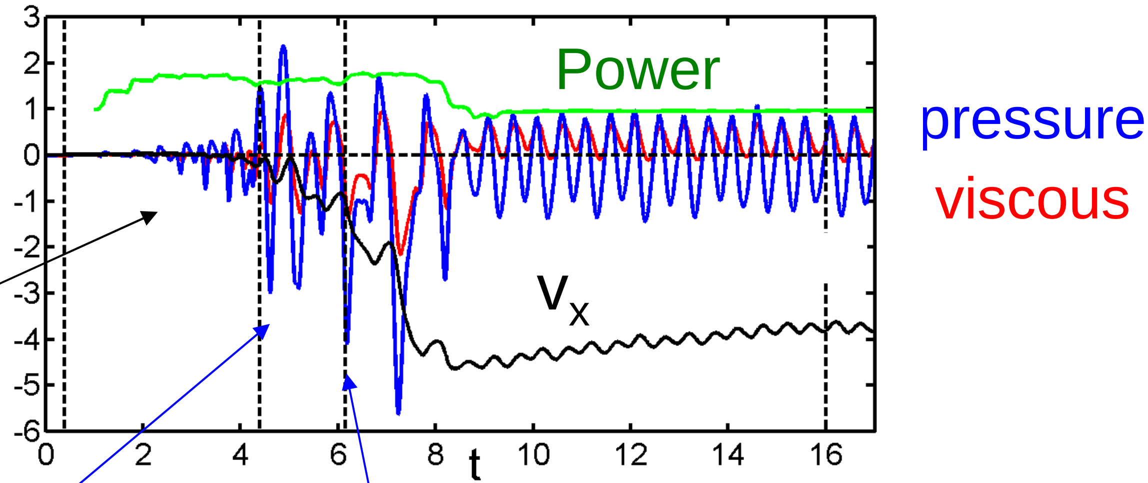

Exponential growth of small perturbations

Flow asymmetry O(1)
$v_x << 1$

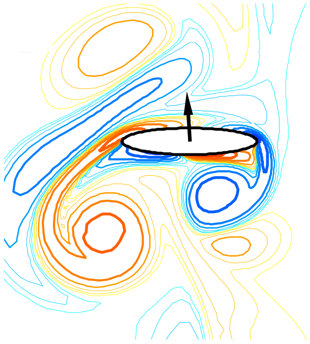

…punctuated by <u>vortex collisions</u>…
v_x becomes O(1)

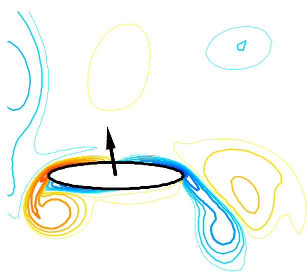

…yielding quasi-steady locomotion.

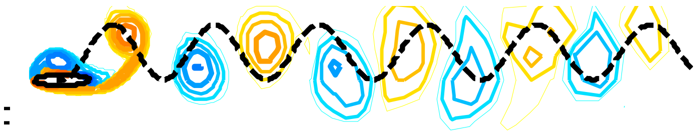

The sequence of events leading to forward flight

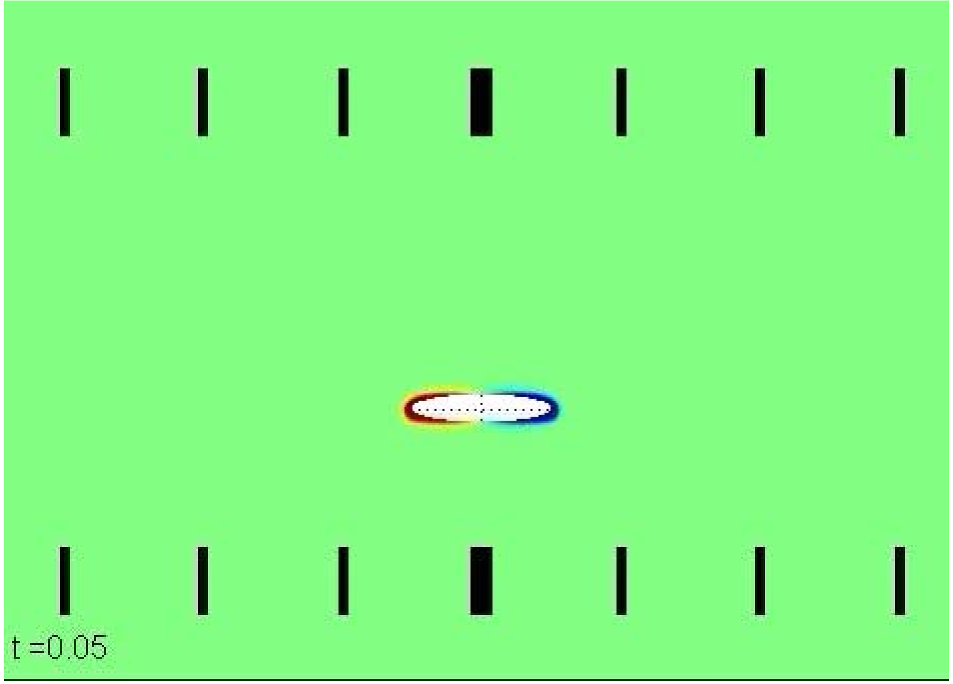

Forward speed (Re_U) vs. flapping speed (Re_f)

$\rho_{body}/\rho_{fluid} = 17$ Aspect ratio 10:1

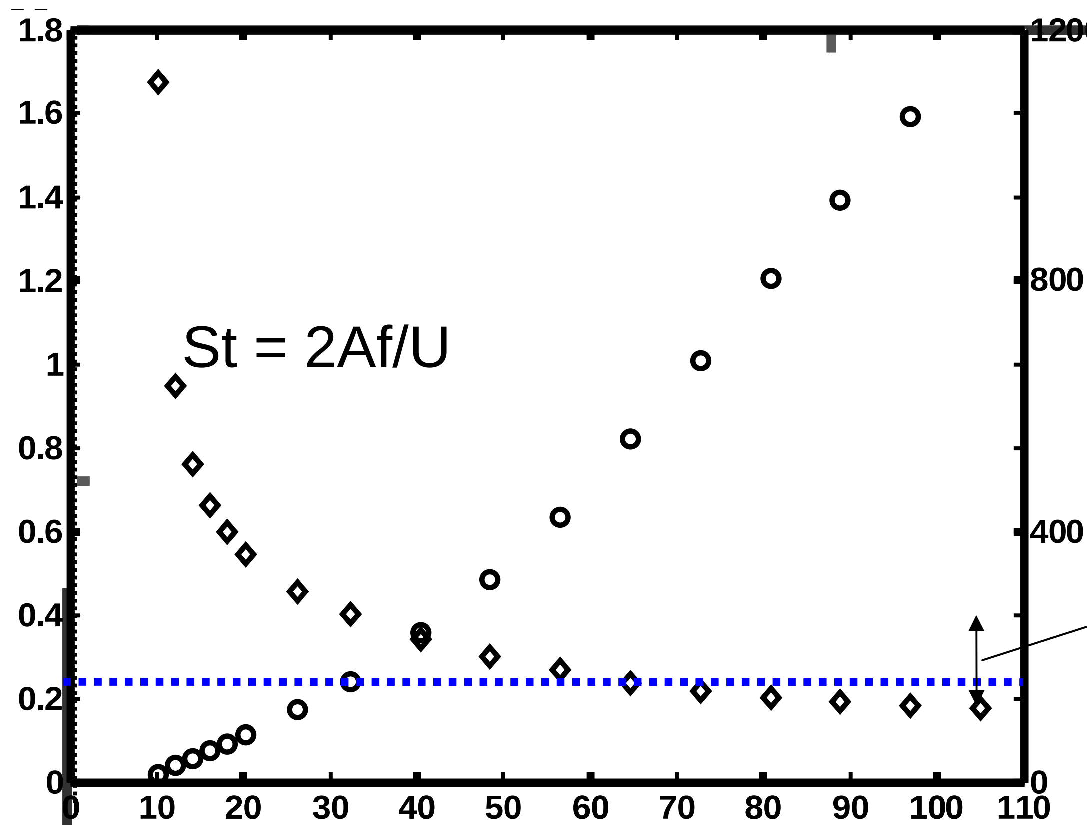

"Optimal efficiency in biology" (G. Taylor et al. Nature '03 711)

Rotary Flapper

Re_{cr} for linear instability

No evidence of bistability

Summary

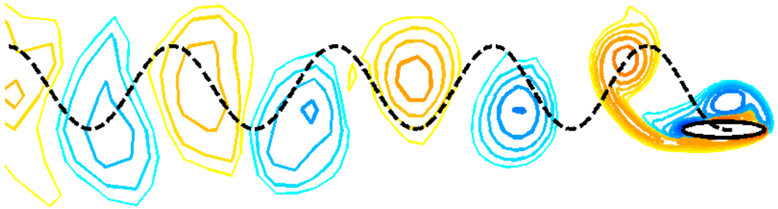

We have explored the threshold Re at which pure heaving generates locomotion

Forward flight at “efficient” St numbers is an attracting state,
for large enough body mass

For smaller masses and thick wings,
phase-locked oscillations (at low Re_f),
and chaotic trajectories (at high Re_f) are seen

A thin wing experiences a smoother start-up, and viscous thrust

The wing “takes off” by colliding with previously-shed vortices

The initial instability is purely fluid-dynamical (von Karman shedding)

Acknowledgements

Michael Shelley (NYU)
Jun Zhang (NYU)
Stephen Childress (NYU)
Nicolas Vandenberghe (IRPHE)

DOE support